Stem Cell Reports
Report
ISSCR
OPEN ACCESS

Human iPSC-derived salivary gland cell sheets integrate with injured glands to form glandular structures

Erika Matsuno,[1] Junichi Tanaka,[2,5,*] Kazuki Nakashima,[3] Yuri Wada,[4] Shintaro Ohnuma,[2] Rikuo Masuda,[1] and Kenji Mishima[2]

[1]Division of Anesthesiology, Department of Perioperative Medicine, Graduate School of Dentistry, Showa Medical University, Tokyo, Japan
[2]Division of Pathology, Department of Oral Diagnostic Sciences, Graduate School of Dentistry, Showa Medical University, Tokyo, Japan
[3]Department of Oral and Maxillofacial Surgery, Graduate School of Dentistry, Showa Medical University, Tokyo, Japan
[4]Department of Orthodontics, Graduate School of Dentistry, Showa Medical University, Tokyo, Japan
[5]Lead contact
*Correspondence: jtanaka@dent.showa-u.ac.jp
https://doi.org/10.1016/j.stemcr.2025.102674

SUMMARY

Functional integration of transplanted cells with host tissue remains a major challenge in cell-based therapies for tissue damage in organs with complex structures, such as exocrine glands. In this study, we investigated whether salivary gland organoids derived from human induced pluripotent stem cells (hiPSCs) could be integrated into injured salivary glands using cell sheet engineering. Cell sheet engineering has demonstrated therapeutic potential in a range of organs, including the heart, retina, and lungs. We found that hiPSC-derived salivary gland organoids contain long-term maintainable progenitor cells, and the resulting cell sheets exhibited heterogeneity, including acinar, ductal, and myoepithelial cells. Furthermore, transplantation of the organoid-derived salivary gland cell sheets into immunodeficient mice resulted in partial integration with the host salivary ducts, leading to the formation of structures that included xenogeneic chimeric ducts. These findings suggest that salivary gland cell sheet transplantation represents a promising strategy for functional salivary gland regeneration.

INTRODUCTION

Salivary gland dysfunction caused by radiotherapy for head and neck cancer or Sjögren syndrome leads to xerostomia, resulting in significant oral dysfunction (Jensen et al., 2019). Cell therapy shows potential as a novel therapeutic approach for these conditions to restore the glandular tissue, with ongoing clinical trials focusing on adult stem-cell-derived salivary gland organoids (Verstegen et al., 2025). Proper maintenance of the ductal structures necessary for salivary secretion into the oral cavity remains a major challenge for the development of effective regenerative therapies for salivary gland dysfunction. Transplanted cells must not only engraft but also establish a functional connection with the host ductal system to contribute to salivary flow. Effective coordination between host tissue architecture and transplanted cells remains a universal challenge in organoid-based transplantation therapies (van den Berg et al., 2025; Qi et al., 2024; Thompson and Takebe, 2021). Recently, functional integration of human cells into the mouse liver has been reported (Igarashi et al., 2025; Reza et al., 2025). However, in the context of cell transplantation into salivary glands, the mechanisms by which transplanted cells integrate with the host tissue structures to ensure functional recovery remain unclear.

Previously, we successfully generated human salivary gland organoids from induced pluripotent stem cells (iPSCs) and transplanted them into immunodeficient mice following the removal of parotid glands, thereby maintaining a salivary secretion pathway into the oral cavity (Tanaka et al., 2022). However, this transplantation method requires the complete removal of the host salivary glands (Ogawa et al., 2013; Tanaka et al., 2018). Clinically, new methods are urgently needed for the transplantation of donor cells, while preserving the host salivary glands and facilitating their integration. To date, functional integration through expansion and transplantation of organoids derived from mouse salivary gland tissue has been demonstrated (Hong et al., 2022; Maimets et al., 2016; Xiao et al., 2014). However, reports on the transplantation outcomes of salivary gland organoids derived from human salivary gland tissue remain limited (Jeon et al., 2024; Pringle et al., 2016). A recent study reported the transplantation of organoids derived from dissociated human salivary gland tissues into immunodeficient mice (Jeon et al., 2024). It has been reported that, following transplantation of human salivary gland organoids into immunodeficient mice, the transplanted organoids produce mucin within the mouse salivary gland tissue. However, the transplanted cells formed structures independent of the recipient ductal system.

Cell sheet technology using temperature-responsive dishes is a potential method for cell transplantation into injured tissues (Yamato and Okano, 2004). A major advantage of temperature-responsive dishes is that the cultured cells are harvested as intact sheets along with their extracellular matrix by simply lowering the temperature, without the need for proteolytic enzymes. This non-invasive

harvesting method has been shown in studies of other organs to allow transplantation while preserving cell-cell junctions and extracellular matrix proteins of the cultured cells (Sekine et al., 2011). Moreover, cell sheets generated from dissociated mouse salivary gland tissues restore the damaged salivary gland tissues (Dos Santos et al., 2020; Nam et al., 2019). However, the precise mechanisms by which the transplanted cells influence the host salivary gland remain unclear. While salivary gland cell sheet transplantation represents a promising strategy for the repair of damaged salivary tissues, further investigation is needed to clarify the direct contribution of the transplanted cells and validate this approach using human cells.

In this study, we successfully generated salivary gland cell sheets containing both ductal and acinar cells using the organoids. Furthermore, transplantation of these cell sheets into the damaged salivary glands of mice revealed the seamless integration of human salivary gland structures with the host ductal structures.

RESULTS

hiPSC-derived salivary gland organoids contain continuous organoid-forming cells

We investigated whether the functionality of the human iPSC (hiPSC)-derived salivary gland organoids generated using our previously reported 80-days differentiation protocol (Tanaka et al., 2022) can be maintained over time. To monitor the salivary gland architecture, we established aquaporin 5 (AQP5) reporter hiPSCs using the CRISPR/Cas9 system. We designed single guide RNAs (sgRNAs) targeting the region upstream of the stop codon in AQP5 and synthesized donor ssDNA (Figure 1A). Genomic PCR analysis of the clones isolated from these neomycin-resistant colonies confirmed the insertion of EGFP downstream of AQP5, and Sanger sequencing further validated this in-frame insertion (Figure S1A). The generated AQP5::EGFP hiPSCs enabled the differentiation of AQP5-positive proacinar cells during salivary gland organoid induction (Figure 1B). Indeed, salivary-gland-like structures with branched morphology developed at the periphery of AQP5-EGFP hiPSC-derived organoids at day 60 (D60) of differentiation, and EGFP signals were observed in these regions (Figure 1C, arrowhead). Salivary gland organoids derived from AQP5 reporter iPSCs showed highly overlapping patterns of HA and AQP5 antibody-positive cells upon fluorescence staining, confirming the proper functioning of the reporter cells (Figure S1B). Additionally, in the salivary gland-like structures showing E-cadherin (E-Cad)-positive epithelial branching morphology, keratin (K)-5- and K14-positive basal cells and α-smooth muscle actin (SMA)-positive myoepithelial cells were arranged with clear polarity, with Ki67-positive proliferating cells primarily detected in the bud region (Figure S1C). Notably, no signal was detected for PAX6, a marker of the lacrimal gland, which is similar to the salivary glands (Figure S1C). Furthermore, after isolation, the entire organoid was purified into a branched structure with EGFP on D80 (Figure 1C).

Next, to examine whether functional stem cells were maintained within the induced gland organoids on D80, we isolated the distal regions and repeatedly passaged them to assess the feasibility of long-term expansion culture (Figure 1D). Even after distal region isolation, the organoids continuously branched and increased in size (Figure 1E). AQP5::EGFP signals corresponding to the end buds were also detected (Figure 1E). Histological analysis revealed that the D120 organoids exhibited a distinct branching structure composed of pan-cytokeratin (Pan-CK)-positive epithelium, with AQP5::HA-positive cells in the distal end buds (Figure 1F). Notably, intracellular localization of AQP5 did not follow the expression patterns observed in mature acinar cells, in which AQP5 aggregated on the luminal side. Instead, it exhibited a developmental pattern characteristic of immature acinar cells, and its expression was also observed on the basolateral cell membranes (Figure 1F). Furthermore, α-SMA-positive myoepithelial and K14-positive basal cells were localized to the spindle-shaped cells on the basal side of the end buds, whereas K19-positive ductal cells were arranged on the luminal side. Ki67-positive proliferating cells were localized to the distal end buds (Figure 1F).

These findings suggest that a cell population capable of continuously forming salivary gland organoids is preserved with embryonic features, even after D80. Moreover, distal region isolation prevents central necrosis and supports the long-term expansion of salivary gland organoids.

Human salivary gland cell sheet generation from iPSC-derived salivary gland organoid

As the induced organoids contained cell populations capable of forming glandular structures, they were dispersed via enzymatic treatment and seeded onto temperature-responsive dishes for cell sheet production for transplantation (Figure 2A). The seeded cells adhered to the dish without the need for special coating and proliferated into sheets, reaching confluency 5 days after seeding (Figure 2B). Upon decreasing the temperature of the confluent culture dish, the cells detached from the dish in a sheet-like form and were subsequently collected (Figure 2B). Fluorescence images revealed that some cells formed AQP5::EGFP-positive clusters despite flat culture conditions (Figure 2C). Histological analysis was performed to examine the cell types in the sheets. The cell sheets consisted of approximately three cell layers, including a population of AQP5-positive cells (Figures 2D and 2E). Almost all

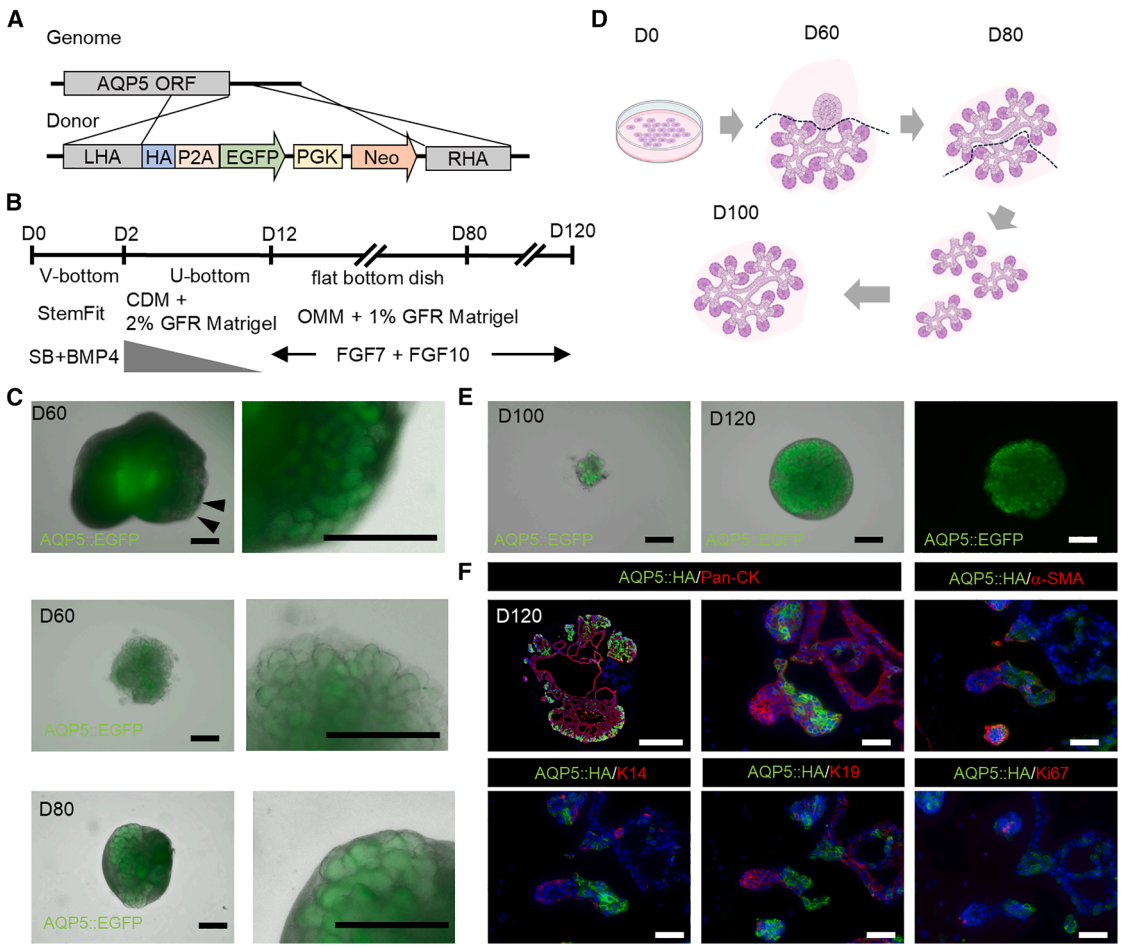

Figure 1. Long-term expansion culture of human induced pluripotent stem cell (hiPSC)-derived salivary gland organoids

(A) Establishment of aquaporin 5 (AQP5) reporter hiPSCs using the CRISPR/Cas9 system. Endogenous AQP5 tagged with hemagglutinin (HA) and enhanced green fluorescent protein (EGFP) was linked to AQP5 using a P2A peptide.

(B) Differentiation protocol for salivary gland organoids derived from hiPSCs. On D60, D80, and D100, branching structures were manually isolated for long-term culture.

(C) Comparison before and after the isolation of the branching region of AQP5::EGFP hiPSCs (D60). Arrowheads indicate the regions of branching structures and their magnified views (top). After isolation, EGFP signals were observed throughout the entire bud region (middle). At D80, the salivary gland organoids consisted exclusively of branching structures with AQP5::GFP-positive terminal buds (bottom left). A magnified view of the branching structure is shown (bottom right). Scale bars, 500 μm.

(D) Schema for the long-term culture of human salivary gland organoids: the organoids on D80 were manually divided and continued in floating culture, after which division was performed once every 20 days for long-term expansion culture.

(E) Divided salivary gland organoids on D100 (left). Organoids on D120 of continuous floating culture after dividing are shown (middle and right). Scale bars, 500 μm.

(F) Immunofluorescence analysis of salivary gland marker protein and HA for AQP5 detection in organoids on D120. Scale bars, 500 μm (left) and 50 μm (others; $n = 3$ biological replicates from three individual experiments).

cells comprising the sheets were positive for pan-cytokeratin (Pan-CK) and E-Cad, indicating their epithelial identity (Figure 2F). These cells expressed SOX9, a transcription factor found in the salivary glands, and were predominantly positive for K5, a basal cell marker, and K14 (Figure 2G). However, some cells expressed K19, K13, and K8, which are typically found in luminal cells of the duct (Figures 2G and S2A). The majority of cells in the salivary gland cell sheet express K5 and K14, with a subset also expressing K19, suggesting that these cells exhibit a gene expression pattern resembling that of embryonic salivary gland ducts (Hauser et al., 2020; Lombaert et al., 2013; Sekiguchi et al., 2020). Only a few cells expressed the myoepithelial marker, α-SMA, and Ki67 staining revealed that both AQP5-positive

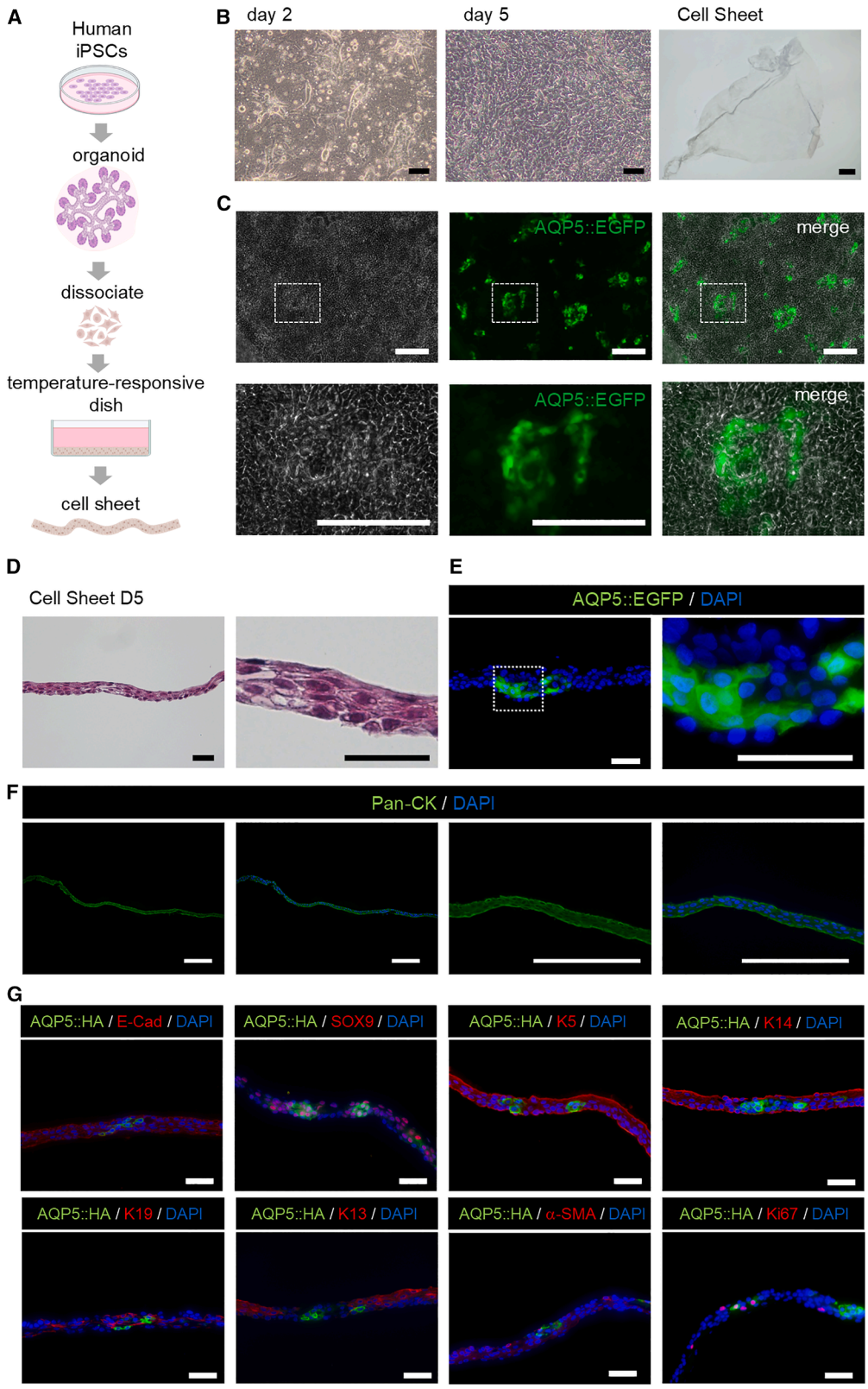

(legend on next page)

and AQP5-negative cells retained their proliferative capacity (Figure 2F). Although the salivary gland cell sheets contained the salivary gland constituent cells, no ZO-1-positive lumen formation was detected (Figure S2A). RT-qPCR revealed that the acinar markers SOX10 and AQP5, ductal marker keratin 19 (KRT19), basal cell marker KRT5, and myoepithelial marker ACTA2 maintained similar expression patterns in the cell sheets and salivary gland organoids (Figure S2B). However, expression levels of the undifferentiated markers, POU5F1 and NANOG, were significantly lower than those in hiPSCs (Figure S2B). Collectively, these results suggest that salivary-gland-organoid-derived cell sheets composed of heterogeneous salivary gland epithelial cell populations support glandular tissue reconstruction post-transplantation.

Human salivary gland cell sheet transplantation reconstructs the ductal structures in continuity with the host mouse ductal system

To evaluate their ability to integrate with the host tissues after transplantation, the cell sheets were transplanted into immunodeficient mice with damaged salivary glands (Figure 3A). The transplantation procedure and the timing of analysis were determined based on previously published studies, and the analysis was conducted one month after transplantation (Dos Santos et al., 2020; Nam et al., 2019). Briefly, a cervical skin incision was made to expose the salivary glands, and 2-mm hole was created in the submandibular glands using a tissue punch to induce damage. In the transplantation group, salivary gland cell sheets were transplanted into the openings created by the punch (Figure 3B). Under our experimental conditions, no obvious differences in the gross morphology of salivary glands were observed between the sham and injured groups (Figure 3C). In contrast, histological analysis revealed that the injured group exhibited acinar atrophy in the lobule units compared to the sham group (Figure 3D). This atrophy was possibly due to the disruption of ductal continuity caused by the punch procedure. Histological analysis via immunofluorescence staining revealed that the salivary glands in the injured group exhibited lobules with markedly reduced AQP5 levels, consisting predominantly of conduit structures (Figure 4A). Similar atrophic lobules were observed in the transplantation group (Figure 4A). To determine the origin of these irregular gland duct structures observed, staining was performed with mouse-specific EpCAM and human-specific mitochondrial antibodies or human-specific nuclear antibodies (Figure 4B and S3A). Notably, the ductal structures exhibited continuity with regions comprising host-derived salivary gland epithelial cells and human cells originating from the transplanted cell sheets, forming E-Cad-positive interspecific chimeric ducts. Therefore, the transplanted human cells did not engraft as autonomous structures in the host salivary glands but rather contributed to ductal reconstruction in cooperation with the host mouse epithelial cells. Furthermore, human cells within this chimeric duct exhibited double positivity for basal cell marker K5 and ductal cell marker K19. In contrast, luminal cells were negative for K14, whereas basal cells were positive for K14, with some also expressing α-SMA (Figure 4C and S3B). Furthermore, both human and mouse cells within this structure included Ki67-positive proliferating cells (Figure 4C). These findings indicate that human cells were transplanted as salivary gland cell sheets within injured mouse salivary glands. In addition, the engraftment of acinar cell clusters composed of transplanted AQP5::HA-positive cells were infrequently observed (Figure S4A) (one out of eight transplanted mice). These clusters were located near the transplantation site adjacent to K19-positive ductal structures and were accompanied by α-SMA-positive myoepithelial cells (Figure S4B). Moreover, expression of amylase, a digestive enzyme found in saliva, was not detected in these structures (Figure S4C). These findings suggest that the salivary

Figure 2. Generation of salivary gland cell sheets from hiPSCs

(A) Schema for the generation of salivary gland cell sheets.

(B) Phase contrast images of cells derived from the decentralized salivary gland organoids on D2 (left) and D5 (center). Stereomicroscopic image of a detached cell sheet is shown (right). Scale bars, 500 μm (left) and 1 mm (right; n = 12 biological replicates from at least three individual experiments).

(C) Immunofluorescence images of the cell sheets, including a population of AQP5-positive cells. Scale bars, 200 μm (n = 12 biological replicates from at least three individual experiments).

(D) Histological analysis of cell sheets via hematoxylin and eosin staining. Scale bars, 50 μm (n = 3 biological replicates from three individual experiments).

(E) Fluorescence images of AQP5::EGFP reporter hiPSC-derived salivary gland cell sheets after 4′,6-diamidino-2-phenylindole (DAPI) staining. Scale bars, 50 μm (n = 3 biological replicates from three individual experiments).

(F) Immunofluorescence images of the cell sheets, including a population of Pan-CK-positive epithelial cells. Scale bars, 50 μm (n = 3 biological replicates from three individual experiments).

(G) Immunofluorescence analysis of salivary gland marker protein and HA for AQP5 detection in cell sheets. Scale bars, 50 μm (n = 3 biological replicates from three individual experiments).

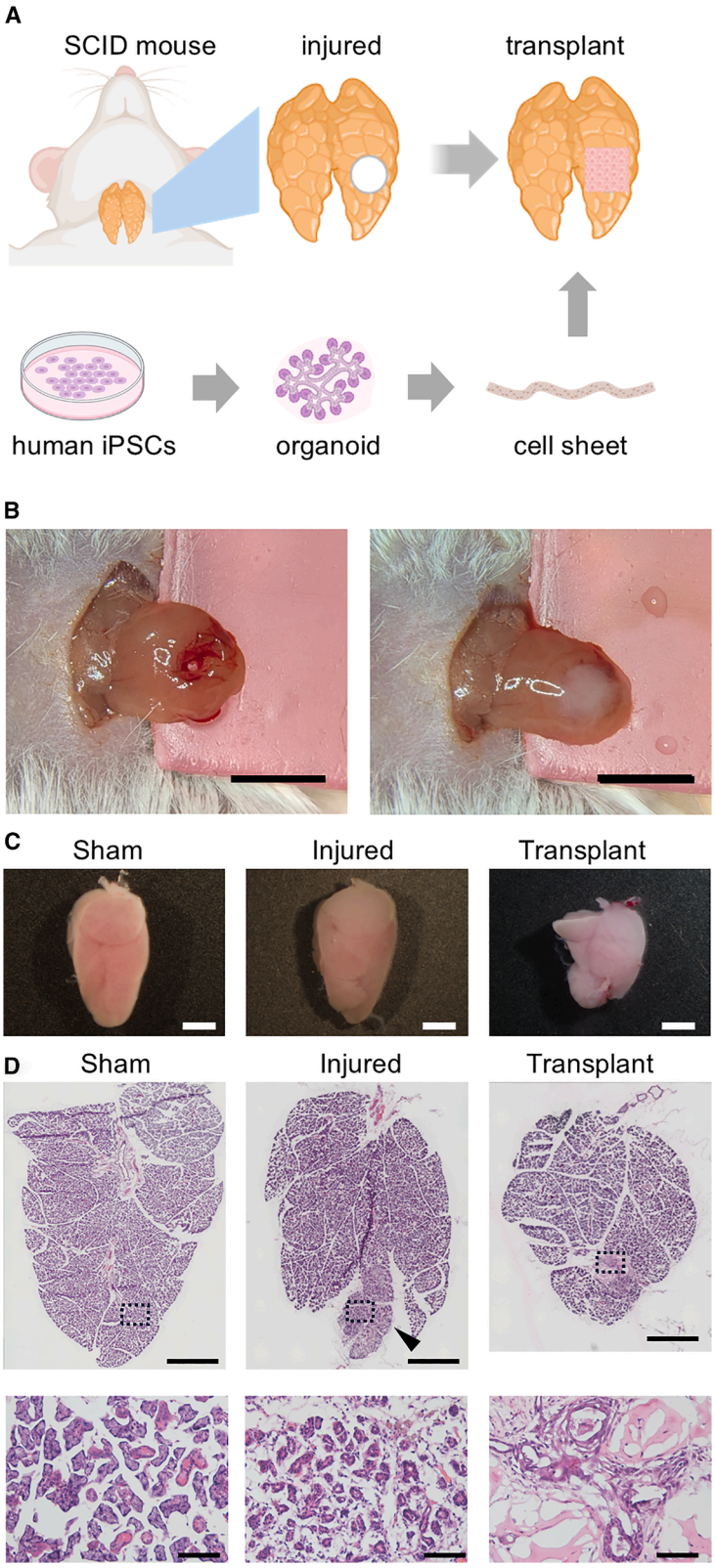

Figure 3. Human salivary gland cell sheet transplantation into the injured salivary glands of immunodeficient mice

(A) Schema for human salivary gland cell sheet transplantation into the injured submandibular glands of immunodeficient mice.

(B) Gross images of the submandibular glands after hole formation via a punch (left) and cell sheet transplantation (right). Scale bars, 5 mm (n = 4 mice/group from three individual experiments).

(C) Stereomicroscopic images of the submandibular and sublingual glands 1 month after treatment of the uninjured sham group (left), injured group with punching treatment without transplantation (middle), and transplanted group with punching treatment and cell sheet transplantation (right). Scale bars, 2 mm (n = 4 mice/group from three individual experiments).

(D) Hematoxylin and eosin staining of the sham, injured, and transplantation groups. The arrowhead indicates the region of atrophic lobules. Scale bars, 500 μm (upper) and 50 μm (lower).

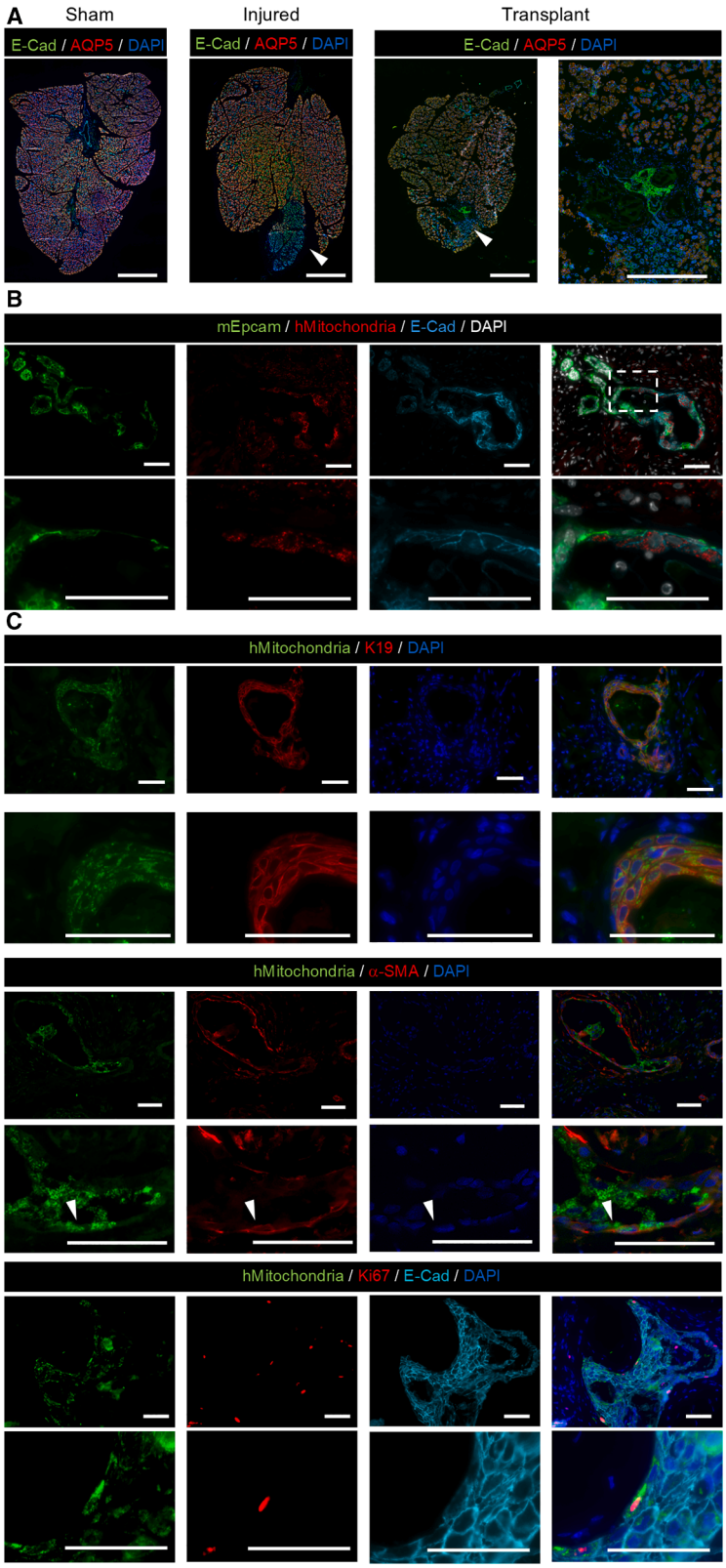

Figure 4. Engrafted human salivary gland cell sheets form glandular structures in coordination with the injured mouse salivary glands

(A) Immunofluorescence images of the sham group (left), injured group (middle), and transplanted group with punching treatment and cell sheet transplantation (right) stained with antibodies against E-cadherin (E-Cad) and AQP5. The arrowhead indicates the region of atrophic lobules. Scale bars, 500 μm.

(B) Immunofluorescence images of human salivary gland cell sheets transplanted into the injured submandibular glands of immunodeficient mice stained with antibodies against mouse-specific epithelial cell adhesion molecule (EpCAM), human-specific mitochondria, and E-Cad. Scale bars, 50 μm.

(C) Immunofluorescence images of human salivary gland cell sheets transplanted into the injured submandibular glands of immunodeficient mice stained with antibodies against salivary gland marker proteins. Scale bars, 50 μm (n = 4 mice/group from three individual experiments).

gland cell sheets may contribute to the regeneration of acinar cells; however, further strategies are needed to promote their maturation.

Overall, transplanted hiPSC-derived salivary gland cell sheets integrated well with the injured host salivary gland ducts at the cellular level, serving as effective transplantation tools for exocrine glands, where ensuring continuity with the host duct system is crucial.

DISCUSSION

In this study, we demonstrated that hiPSC-derived salivary gland organoids retained the ability to form acinar-cell-containing branching structures over the long term. Furthermore, we generated cell sheets containing salivary gland constituent cells from these organoids using temperature-responsive culture dishes and observed human cell engraftment upon xenotransplantation into immunodeficient mice. The transplanted human cells maintained cellular polarity and formed ductal structures that were histologically integrated into the host mouse ducts.

Long-term cultures of organoids derived from tissue stem cells via self-renewal have been established for various organs, such as the intestine, significantly contributing to regenerative medicine and disease research (Sachs et al., 2019; Sato et al., 2009). Several studies have generated human salivary gland organoids from tissue stem cells (Jeon et al., 2024; Lu et al., 2025; Pringle et al., 2016; Yoon et al., 2022). However, unlike mouse salivary gland organoids, human organoids exhibit solid or cystic structures and lack distinct branching phenotypes. These morphological characteristics are consistent with those reported in other stem-cell-derived human exocrine gland organoids (Richards et al., 2019; Rosenbluth et al., 2020). In this study, iPSC-derived human salivary gland organoids were successfully maintained for a long time while retaining their branching phenotype via mechanical passaging. The observed differences in organoid morphology possibly reflect the functional differences between fetal and adult salivary gland stem cells. Consistently, a recent study on pancreas, another organ with a branched structure, demonstrated that organoids retaining a branched morphology can only be established from embryonic pancreatic tissues, whereas those derived from adult pancreatic tissues lack this structure (Andersson-Rolf et al., 2024). These findings suggest the presence of fetal stem cells with tissue-forming potential within iPSC-derived human salivary gland organoids, explaining their resemblance to embryonic salivary glands (Tanaka et al., 2022). However, further research is necessary to elucidate the functional differences between fetal and adult stem cells and their implications for therapeutic applications.

The salivary-gland-organoid-derived cell sheets generated in this study consisted of heterogeneous cell populations, including acinar, ductal, and myoepithelial cells. A previous study developed cell sheets derived from mouse salivary gland tissues and reported limited AQP5-positive cells under monoculture conditions (Nam et al., 2019). This difference was possibly because mature acinar cells are generally vulnerable to stress, such as cell dissociation, and exhibit low engraftment efficiency (van den Brink et al., 2017). Here, hiPSC-derived organoids contained a high proportion of immature proacinar cells, which contributed to their enhanced survival. Histological analysis post-cell sheet transplantation revealed the integration of human salivary gland cell sheets with the host mouse ducts, forming interspecies chimeric ducts. In these human ductal cells, polarity was re-established in both basal and luminal cells. Although previous studies have reported the orthotopic transplantation of organoids derived from human salivary gland tissues, the transplanted cells generally form independent structures within the host salivary glands (Jeon et al., 2024; Lu et al., 2025). The cellular integration observed in this study underscores the advantage of salivary gland cell sheet transplantation, which serves as a novel strategy to combine salivary gland organoids with cell sheets. A limitation of this study is that the engraftment of AQP5-positive acinar-like cells derived from the transplanted hiPSC-derived organoid cell sheets was limited, and no amylase expression was detected. To restore salivary secretion, efficient reconstruction of functional acinar structures after transplantation is essential. Given the difficulty in maintaining differentiated acinar cells in culture, future studies should focus on modifying the culture conditions to develop cell sheets containing cells in a progenitor-like state to enhance acinar cell engraftment.

METHODS

Differentiation of salivary gland organoid from human iPSCs

hiPSCs were dissociated using StemPro Accutase, resuspended in StemFit AK02N medium supplemented with 20 μM Y27632, and seeded at a density of 5,000 cells per well in PrimeSurface 96-well V-bottom plates (Sumitomo Bakelite) with 100 μL per well. On D2, aggregates were transferred to chemically defined medium (CDM) and cultured in Nunclon Sphera 96-well U-bottom low-attachment plates (Thermo Fisher Scientific). CDM consisted of 1% chemically modified lipid concentrate (Thermo Fisher Scientific), 450 μM monothioglycerol (MERCK), 5 mg/mL crystallized bovine serum albumin (MERCK), 2% growth factor-reduced Matrigel (BD Biosciences), and a 1:1 mixture of Iscove's modified Dulbecco's medium and Ham's F-12

(Thermo Fisher Scientific), supplemented with 10 μM SB431542 (Stemgent) and 10 ng/mL BMP4 (PeproTech). On D6 and D8, 25 μL or 75 μL of medium was added, respectively. On D12, aggregates were washed and transferred to 6-cm low-attachment dishes (Nunc) containing organoid maturation medium (OMM). OMM included 0.5% N2 supplement, 1% B27 supplement minus vitamin A, 1 mM penicillin-streptomycin, 1% GlutaMAX (all from Thermo Fisher Scientific), 1% growth-factor-reduced Matrigel, and advanced DMEM/F-12 supplemented with 100 ng/mL FGF7 (R&D Systems) and 200 ng/mL FGF10 (Qkine). On D60, branching structures were manually isolated using a 29-G needle. On D80, AQP5-GFP-positive structures were dissected into smaller fragments using the same method. OMM was refreshed every other day during floating culture. The distinction between EGFP and autofluorescence in the induced organoids was confirmed by histological analysis.

Cell sheet preparation

Organoids were washed with cold PBS, and six organoids were collected and digested in 2 mL of pre-warmed TrypLE Express at 37°C for 60 min with pipetting every 20 min. Digestion was stopped by adding 2 mL of DMEM +10% FBS, and cells were pelleted (300 × g, 3 min). Cells were resuspended in medium containing 100 ng/mL FGF7, 200 ng/mL FGF10, 10 ng/mL EGF, and 10 μM Y27632 and seeded into two wells of a 12-well UpCell temperature responsive plate (Thermo Fisher Scientific). Cultures were maintained at 37°C in 95% air and 5% CO_2, with medium changed every other day. After 5 days, the temperature was lowered to below 25°C, and a cell shifter was applied to harvest intact cell sheets.

Statistics

Statistical analysis was conducted using one-way ANOVA followed by Tukey's post hoc test for multiple comparisons. All analyses were performed using R Studio. Immunofluorescence experiments were independently repeated at least three times with consistent results. No statistical method was used to predetermine sample size, and experiments were not randomized.

RESOURCE AVAILABILITY

Lead contact

Requests for further information and resources should be directed to and will be fulfilled by the lead contact, Junichi Tanaka (jtanaka@dent.showa-u.ac.jp).

Materials availability

Materials used in this study are available from the lead contact, Junichi Tanaka, upon request.

Data and code availability

This study did not generate any unique dataset and original code. Any additional information required to reanalyze the data reported in this paper is available from the lead contact upon request.

ACKNOWLEDGMENTS

This work was supported by JSPS KAKENHI (grant numbers: 23K27780 and 21KK0290 to J.T. and 23K24522 to K.M.) and AMED (grant number: 24bm1123060h0001 to J.T.).

AUTHOR CONTRIBUTIONS

Conceptualization, J.T. and K.M.; methodology, E.M. and J.T.; investigation, E.M., J.T., K.N., Y.W., and S.O.; writing—original draft, E.M., J.T., and K.M.; writing—review & editing, E.M., J.T., and K.M.; supervision, R.M. and K.M.; project administration, J.T. and K.M.; funding acquisition, J.T. and K.M.

DECLARATION OF INTERESTS

The authors declare no competing interests.

SUPPLEMENTAL INFORMATION

Supplemental information can be found online at https://doi.org/10.1016/j.stemcr.2025.102674.

Received: May 16, 2025
Revised: September 9, 2025
Accepted: September 9, 2025
Published: October 9, 2025

REFERENCES

Andersson-Rolf, A., Groot, K., Korving, J., Begthel, H., Hanegraaf, M.A.J., VanInsberghe, M., Salmén, F., van den Brink, S., Lopez-Iglesias, C., Peters, P.J., et al. (2024). Long-term in vitro expansion of a human fetal pancreas stem cell that generates all three pancreatic cell lineages. Cell *187*, 7394–7413.e22. https://doi.org/10.1016/j.cell.2024.10.044.

van den Berg, C.W., Dumas, S.J., Little, M.H., and Rabelink, T.J. (2025). Challenges in maturation and integration of kidney organoids for stem cell-based renal replacement therapy. Kidney Int. *107*, 262–270.

van den Brink, S.C., Sage, F., Vértesy, Á., Spanjaard, B., Peterson-Maduro, J., Baron, C.S., Robin, C., and van Oudenaarden, A. (2017). Single-cell sequencing reveals dissociation-induced gene expression in tissue subpopulations. Nat. Methods *14*, 935–936.

Dos Santos, H.T., Kim, K., Okano, T., Camden, J.M., Weisman, G. A., Baker, O.J., and Nam, K. (2020). Cell sheets restore secretory function in wounded mouse submandibular glands. Cells *9*, 2645.

Hauser, B.R., Aure, M.H., Kelly, M.C., Genomics and Computational Biology Core, Hoffman, M.P., and Chibly, A.M. (2020). Generation of a Single-Cell RNAseq Atlas of Murine Salivary Gland Development. iScience *23*, 101838. https://doi.org/10.1016/J.ISCI.2020.101838.

Hong, H.J., Cho, J.-M., Yoon, Y.-J., Choi, D., Lee, S., Lee, H., Ahn, S., Koh, W.-G., and Lim, J.-Y. (2022). Thermoresponsive fiber-based microwells capable of formation and retrieval of salivary gland stem cell spheroids for the regeneration of irradiation-damaged salivary glands. J. Tissue Eng. *13*, 20417314221085645.

Igarashi, R., Oda, M., Okada, R., Yano, T., Takahashi, S., Pastuhov, S., Matano, M., Masuda, N., Togasaki, K., Ohta, Y., et al. (2025). Generation of human adult hepatocyte organoids with metabolic functions. Nature *641*, 1248–1257.

Jensen, S.B., Vissink, A., Limesand, K.H., and Reyland, M.E. (2019). Salivary gland hypofunction and xerostomia in head and neck radiation patients. J. Natl. Cancer Inst. Monogr. *2019*, lgz016.

Jeon, S.G., Lee, J., Lee, S.J., Seo, J., Choi, J., Bae, D.H., Chun, D.-H., Ko, S.Y., Shin, H.S., Joo, L., et al. (2024). Salivary gland organoid transplantation as a therapeutic option for radiation-induced xerostomia. Stem Cell Res. Ther. *15*, 265.

Lombaert, I.M.A., Abrams, S.R., Li, L., Eswarakumar, V.P., Sethi, A. J., Witt, R.L., and Hoffman, M.P. (2013). Combined KIT and FGFR2b signaling regulates epithelial progenitor expansion during organogenesis. Stem Cell Rep. *1*, 604–619.

Lu, E., Qian, J., Liang, W., Xiang, H., Ding, P., Jin, M., Lin, Z., Chen, Y., Wang, Z., Huang, X., et al. (2025). Establishment of human minor salivary gland organoids in laminin-GelMA hydrogel from healthy individuals and Sjögren's disease patients. Chem. Eng. J. *503*, 158257.

Maimets, M., Rocchi, C., Bron, R., Pringle, S., Kuipers, J., Giepmans, B.N.G., Vries, R.G.J., Clevers, H., de Haan, G., van Os, R., and Coppes, R.P. (2016). Long-term in vitro expansion of salivary gland stem cells driven by Wnt signals. Stem Cell Rep. *6*, 150–162.

Nam, K., Kim, K., Dean, S.M., Brown, C.T., Davis, R.S., Okano, T., and Baker, O.J. (2019). Using cell sheets to regenerate mouse submandibular glands. NPJ Regen. Med. *4*, 16.

Ogawa, M., Oshima, M., Imamura, A., Sekine, Y., Ishida, K., Yamashita, K., Nakajima, K., Hirayama, M., Tachikawa, T., and Tsuji, T. (2013). Functional salivary gland regeneration by transplantation of a bioengineered organ germ. Nat. Commun. *4*, 2498. https://doi.org/10.1038/ncomms3498.

Pringle, S., Maimets, M., Van Der Zwaag, M., Stokman, M.A., Van Gosliga, D., Zwart, E., Witjes, M.J.H., De Haan, G., Van Os, R., and Coppes, R.P. (2016). Human salivary gland stem cells functionally restore radiation damaged salivary glands. Stem Cell. *34*, 640–652.

Qi, J., Zhang, L., Wang, X., Chen, X., Li, Y., Wang, T., Wu, P., and Chai, R. (2024). Modeling, applications and challenges of inner ear organoid. Smart Med. *3*, e20230028.

Reza, H.A., Santangelo, C., Iwasawa, K., Reza, A.A., Sekiya, S., Glaser, K., Bondoc, A., Merola, J., and Takebe, T. (2025). Multizonal liver organoids from human pluripotent stem cells. Nature *641*, 1258–1267. https://doi.org/10.1038/s41586-025-08850-1.

Richards, Z., McCray, T., Marsili, J., Zenner, M.L., Manlucu, J.T., Garcia, J., Kajdacsy-Balla, A., Murray, M., Voisine, C., Murphy, A. B., et al. (2019). Prostate stroma increases the viability and maintains the branching phenotype of human prostate organoids. iScience *12*, 304–317.

Rosenbluth, J.M., Schackmann, R.C.J., Gray, G.K., Selfors, L.M., Li, C.M.-C., Boedicker, M., Kuiken, H.J., Richardson, A., Brock, J., Garber, J., et al. (2020). Organoid cultures from normal and cancer-prone human breast tissues preserve complex epithelial lineages. Nat. Commun. *11*, 1711.

Sachs, N., Papaspyropoulos, A., Zomer-van Ommen, D.D., Heo, I., Böttinger, L., Klay, D., Weeber, F., Huelsz-Prince, G., Iakobachvili, N., Amatngalim, G.D., et al. (2019). Long-term expanding human airway organoids for disease modeling. EMBO J. *38*, e100300.

Sato, T., Vries, R.G., Snippert, H.J., van de Wetering, M., Barker, N., Stange, D.E., van Es, J.H., Abo, A., Kujala, P., Peters, P.J., and Clevers, H. (2009). Single Lgr5 stem cells build crypt-villus structures in vitro without a mesenchymal niche. Nature *459*, 262–265.

Sekiguchi, R., Martin, D., and Genomics and Computational Biology Core, and Yamada, K.M. (2020). Single-Cell RNA-seq Identifies Cell Diversity in Embryonic Salivary Glands. J. Dent. Res. *99*, 69–78.

Sekine, H., Shimizu, T., Dobashi, I., Matsuura, K., Hagiwara, N., Takahashi, M., Kobayashi, E., Yamato, M., and Okano, T. (2011). Cardiac cell sheet transplantation improves damaged heart function via superior cell survival in comparison with dissociated cell injection. Tissue Eng. Part A *17*, 2973–2980.

Tanaka, J., Ogawa, M., Hojo, H., Kawashima, Y., Mabuchi, Y., Hata, K., Nakamura, S., Yasuhara, R., Takamatsu, K., Irié, T., et al. (2018). Generation of orthotopically functional salivary gland from embryonic stem cells. Nat. Commun. *9*, 4216. https://doi.org/10.1038/S41467-018-06469-7.

Tanaka, J., Senpuku, H., Ogawa, M., Yasuhara, R., Ohnuma, S., Takamatsu, K., Watanabe, T., Mabuchi, Y., Nakamura, S., Ishida, S., et al. (2022). Human induced pluripotent stem cell-derived salivary gland organoids model SARS-CoV-2 infection and replication. Nat. Cell Biol. *24*, 1595–1605.

Thompson, W.L., and Takebe, T. (2021). Human liver model systems in a dish. Dev. Growth Differ. *63*, 47–58.

Verstegen, M.M.A., Coppes, R.P., Beghin, A., De Coppi, P., Gerli, M. F.M., de Graeff, N., Pan, Q., Saito, Y., Shi, S., Zadpoor, A.A., and van der Laan, L.J.W. (2025). Clinical applications of human organoids. Nat. Med. *31*, 409–421.

Xiao, N., Lin, Y., Cao, H., Sirjani, D., Giaccia, A.J., Koong, A.C., Kong, C.S., Diehn, M., and Le, Q.-T. (2014). Neurotrophic factor GDNF promotes survival of salivary stem cells. J. Clin. Investig. *124*, 3364–3377.

Yamato, M., and Okano, T. (2004). Cell sheet engineering. Mater. Today *7*, 42–47.

Yoon, Y.-J., Kim, D., Tak, K.Y., Hwang, S., Kim, J., Sim, N.S., Cho, J.-M., Choi, D., Ji, Y., Hur, J.K., et al. (2022). Salivary gland organoid culture maintains distinct glandular properties of murine and human major salivary glands. Nat. Commun. *13*, 3291.